Supporting information

Silver-Driven Coordination Self-Assembly of Tetraphenylethene Stereoisomer: Construct Charming Topologies and their Mechanochromic Behaviors

Yonggang Shi‡, Zhixiang Lu‡, Liyan Zheng*and Qiu-E Cao*

Key Laboratory of Medicinal Chemistry for Natural Resource, Ministry of Education, Functional Molecules Analysis and Biotransformation Key Laboratory of Universities in Yunnan Province, School of Chemical Science and Technology, Yunnan University, Kunming 650091, People's Republic of China.
E-mail: zhengliyan@ynu.edu.cn (L. Zheng), qecao@ynu.edu.cn (Q.-E.C.).

Table S1. Spectroscopic data for **TPE-2by-X-*Z*/*E*.**

Name	Treatment	E_m(nm)	Δλ (nm)	Φ_f (%)	τ (ns)	$k_r/10^8(s^{-1})$	$k_{nr}/10^8(s^{-1})$
TPE-2by-1-*E*	Pristine	458	29	10.00	2.89	0.35	3.11
	Grind	487		33.20	4.00	0.83	1.67
TPE-2by-1-*Z*	Pristine	458	30	14.10	3.10	0.46	2.78
	Grind	488		34.00	4.02	0.85	1.64
TPE-2by-2-*E*	Pristine	466	22	19.50	2.98	0.47	2.88
	Grind	488		37.40	4.13	0.90	1.51
TPE-2by-2-*Z*	Pristine	460	29	22.10	3.12	0.71	2.50
	Grind	489		37.70	4.23	0.89	1.47
TPE-2by-3-*E*	Pristine	449	40	27.40	3.07	0.89	2.36
	Grind	489		44.20	4.29	1.03	1.30
TPE-2by-3-*Z*	Pristine	440	56	33.00	3.14	1.04	2.15
	Grind	496		45.50	4.35	1.05	1.25

Table S2. Spectroscopic data for **Ag-TPE-2by-X-*Z*/*E*.**

Name	Treatment	E_m(nm)	Δλ (nm)	Φ_f (%)	τ (ns)	$k_r/10^8(s^{-1})$	$k_{nr}/10^8(s^{-1})$
Ag-TPE-2by-1-*E*	Pristine	450	0	26.76	3.53	0.80	1.94
	Grind	450		26.76	3.53	0.80	1.94
Ag-TPE-2by-1-*Z*	Pristine	-	-	-	-	-	-
	Grind	-	-	-	-	-	-
Ag-TPE-2by-2-*E*	Pristine	465	10	31.07	4.01	0.77	1.71
	Grind	475		29.42	3.88	0.76	1.82
Ag-TPE-2by-2-*Z*	Pristine	468	13	35.82	4.01	0.89	1.59
	Grind	481		35.42	3.89	0.91	1.66
Ag-TPE-2by-3-*E*	Pristine	448	27	32.13	3.61	0.89	1.88
	Grind	475		31.13	3.83	0.81	1.80
Ag-TPE-2by-3-*Z*	Pristine	444	31	31.60	2.99	1.06	2.29
	Grind	475		29.72	3.63	0.82	1.94

Table S3. Partial bond length and bond angle data for **Ag-TPE-2by-1-*E***.

Ag01-O3	2.61(1)	O3-Ag01	2.44(1)
Ag01-N2	2.294(3)	O4-N3	1.30(2)
Ag01-O3	2.44(1)	N1-Ag01	2.231(3)
Ag01-N1	2.231(3)	Ag01-O3	2.61(1)
O3-Ag01-N2	83.3(3)	Ag01-O3-Ag01	105.5(4)
O3-Ag01-O3	74.5(4)	N3-O3-Ag01	141.9(8)
O3-Ag01-N1	144.0(3)	C28-N1-Ag01	122.3(2)
N2-Ag01-O3	112.8(3)	C32- N1-Ag01	118.5(3)
N2-Ag01-N1	127.3(1)	Ag01-N2-C33	122.1(2)
O3-Ag01-N1	104.0(3)	Ag01-N2-C38	120.0(2)
Ag01-O3-N3	102.2(7)	O3-Ag01-O3	74.5(4)
		Ag01-O3-Ag01	105.5(4)

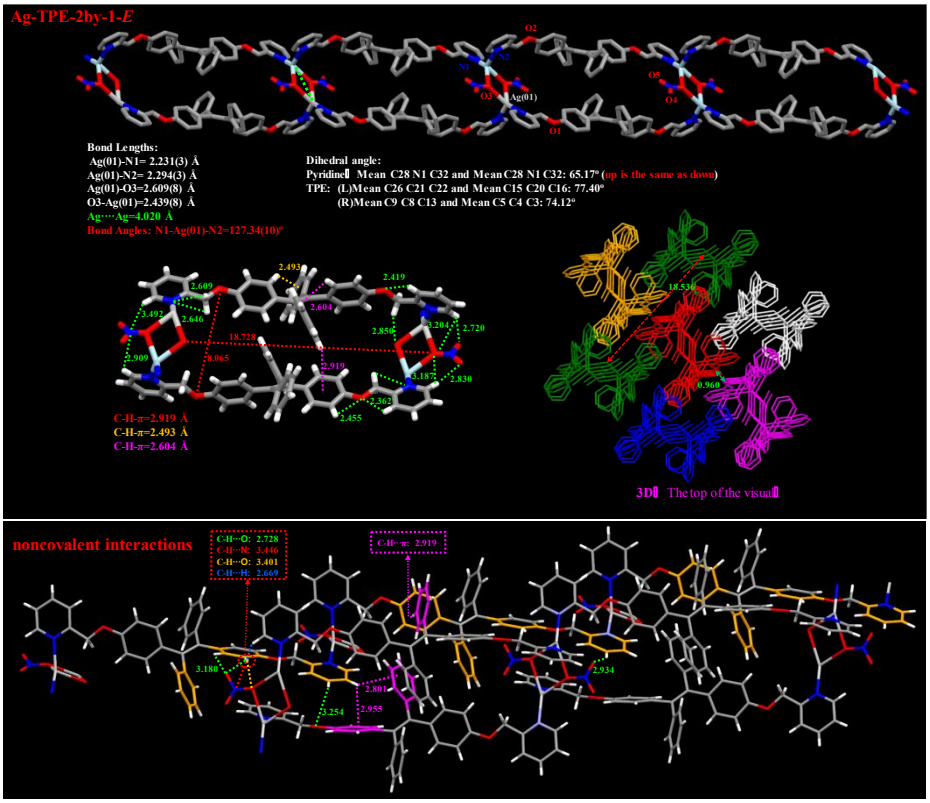

Figure S1. Single crystal structural of **Ag-TPE-2by-1-*E*** and intermolecular noncovalent interactions.

Table S4. Partial bond length and bond angle data for **Ag-TPE-2by-2-*E***.

Ag1-N1	2.156(7)	Ag1-N2	2.182(7)
Ag1-Ag1	3.154(1)	N2-Ag1	2.182(7)
N1-Ag1-Ag1	79.9(2)	Ag1-Ag1-N2	108.1(2)
N1-Ag1-N2	167.2(3)		

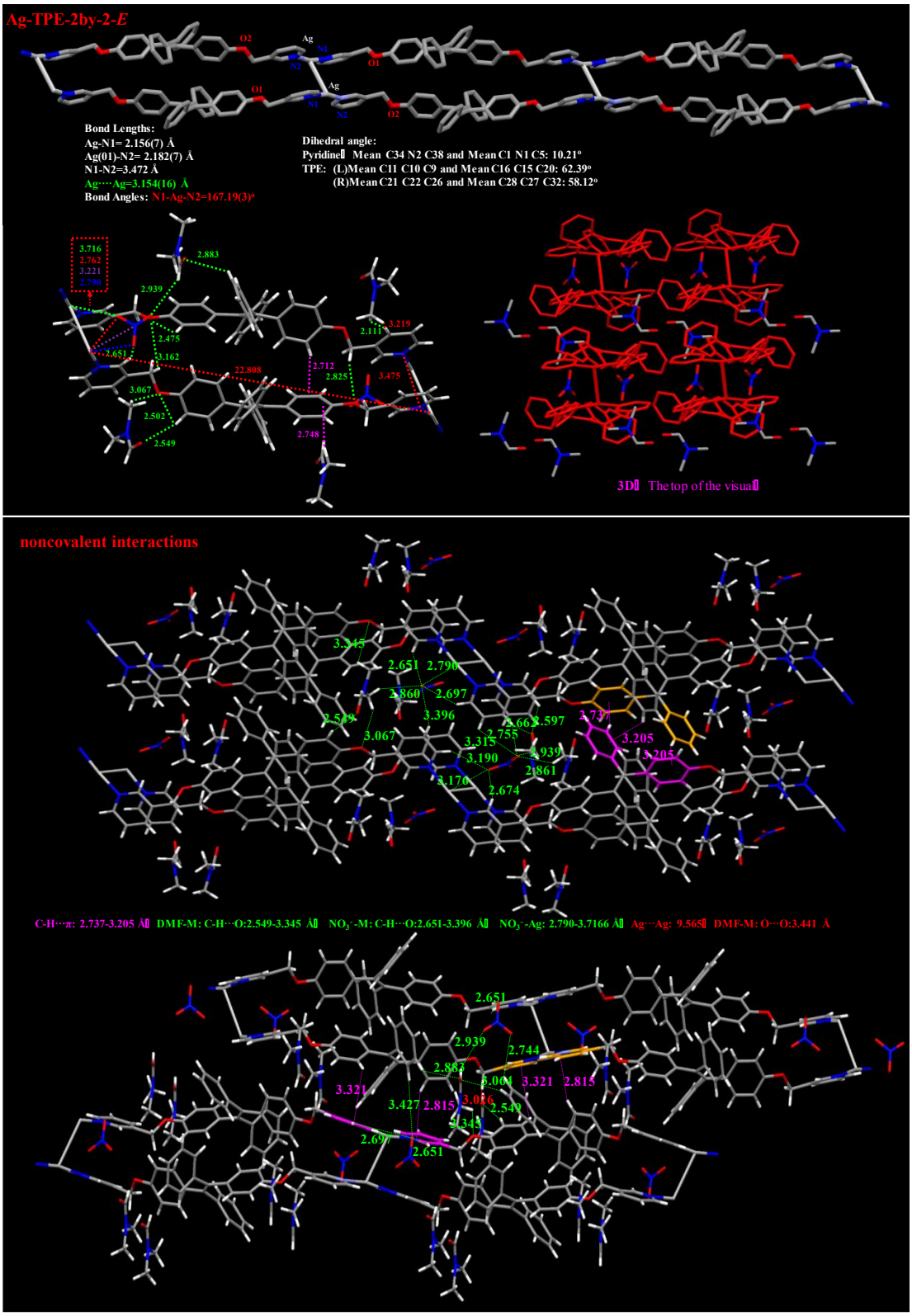

Figure S2. Single crystal structural of **Ag-TPE-2by-2-*E*** and intermolecular noncovalent interactions.

Table S5. Partial bond length and bond angle data for **Ag-TPE-2by-2-*Z***.

Ag1-N4	2.163(4)	Ag2-N1	2.139(4)
Ag1-O8	2.53(1)	Ag2-N3	2.153(4)
Ag1-N2	2.148(5)	Ag2-O5	2.711(6)
N4-Ag1-O8	97.2(3)	Ag2-N1-C5	123.2(3)
N4-Ag1-N2	177.0(2)	Ag2-N3-C38	118.8(3)
O8-Ag1-N2	85.8(3)	Ag2-N3-C42	122.9(3)
N1-Ag2-N3	168.8(1)	Ag1-N4-C74	121.0(4)
N1-Ag2-O5	82.8(2)	Ag1-N4-C75	118.2(3)
N3-Ag2-O5	104.5(2)	Ag2-O5-N5	129.5(4)
Ag2-N1-C1	118.7(3)	Ag1-O8-N6	155(1)

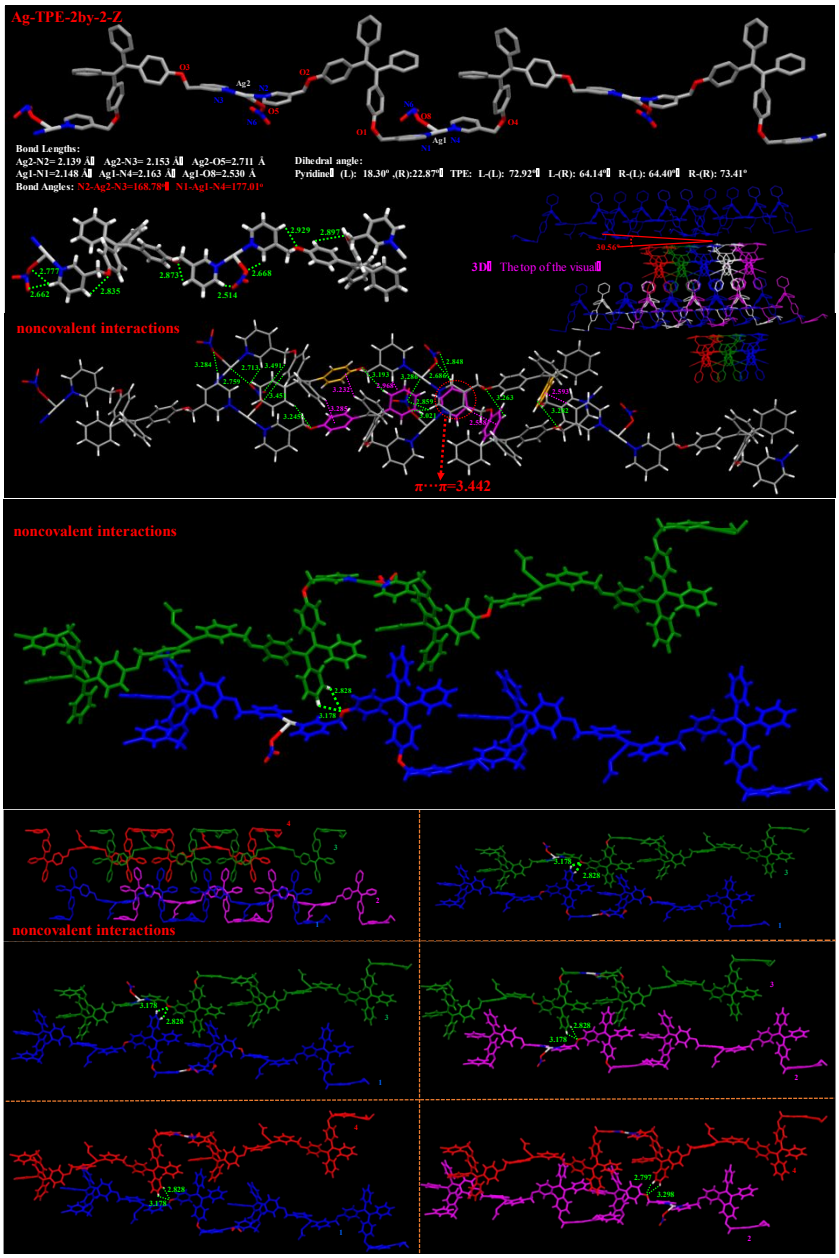

Figure S3. Single crystal structural of **Ag-TPE-2by-2-*Z*** and intermolecular noncovalent interactions.

Table S6. Partial bond length and bond angle data for **Ag-TPE-2by-3-*E***.

Ag1-N1	2.213(7)	Ag1-N2	2.209(7)
Ag1-O4	2.66(2)		
N1-Ag1-O4	89.6(4)	N2-Ag1-O4	91.5(4)
N1-Ag1-N2	161.4(3)	C1-N2-Ag1	123.4(7)
N1-Ag1-O4	88.0(4)	C5-N2-Ag1	118.4(6)
O4-Ag1-N2	109.0(4)	Ag1-O4-N3	101(1)
O4-Ag1-O4	95.9(5)	Ag1-O4-Ag1	84.1(4)
		N3-O4-Ag1	173(1)

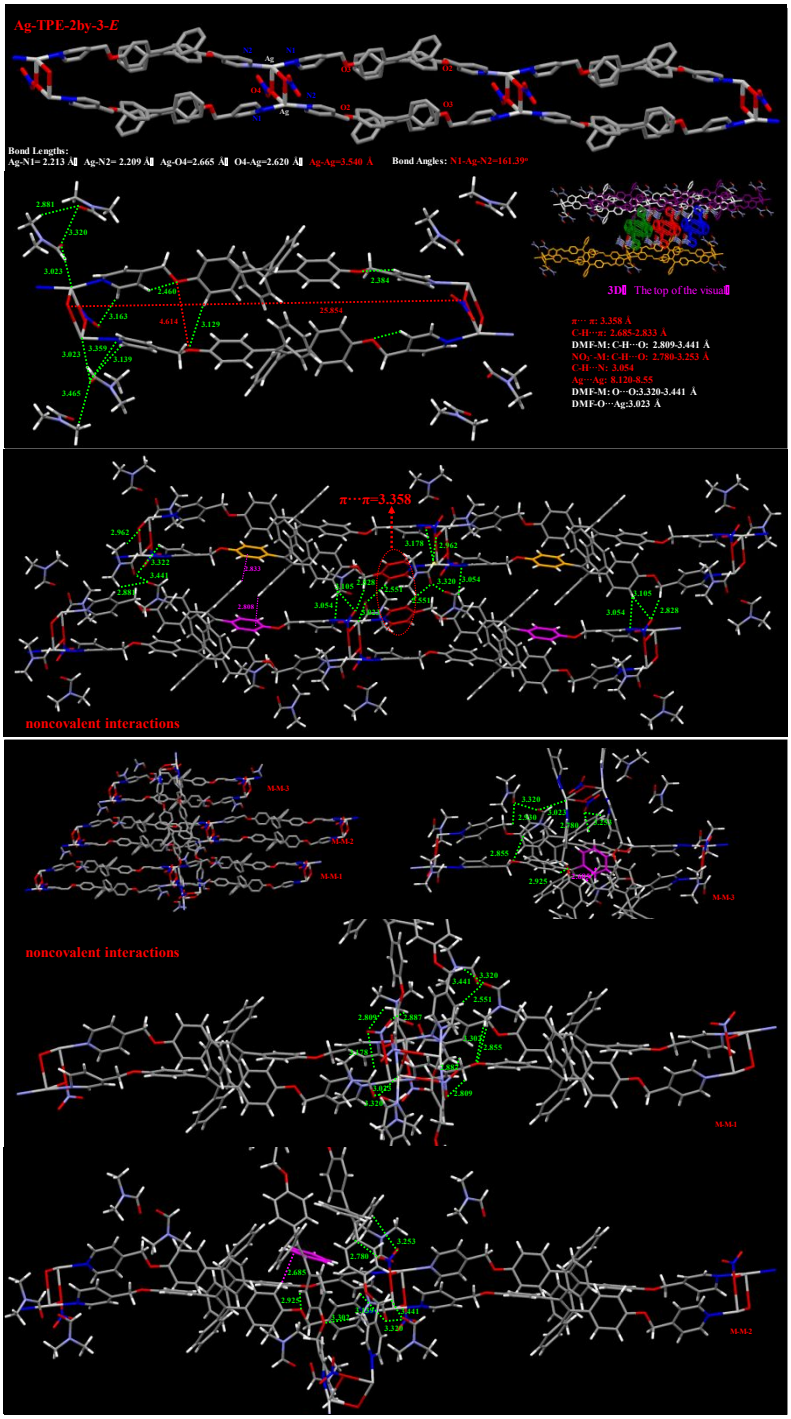

Figure S4. Single crystal structural of **Ag-TPE-2by-3-*E*** and intermolecular noncovalent interactions.

Table S7. Partial bond length and bond angle data for **Ag-TPE-2by-3-*Z***.

Ag1-N1	2.171(8)	Ag1-N2	2.163(8)
C36-N2-Ag1	123.0(7)	N1-Ag1-N2	175.3(3)
C37-N2-Ag1	120.3(7)	Ag1-N1-C2	122.0(7)
		Ag1-N1-C3	120.2(7)

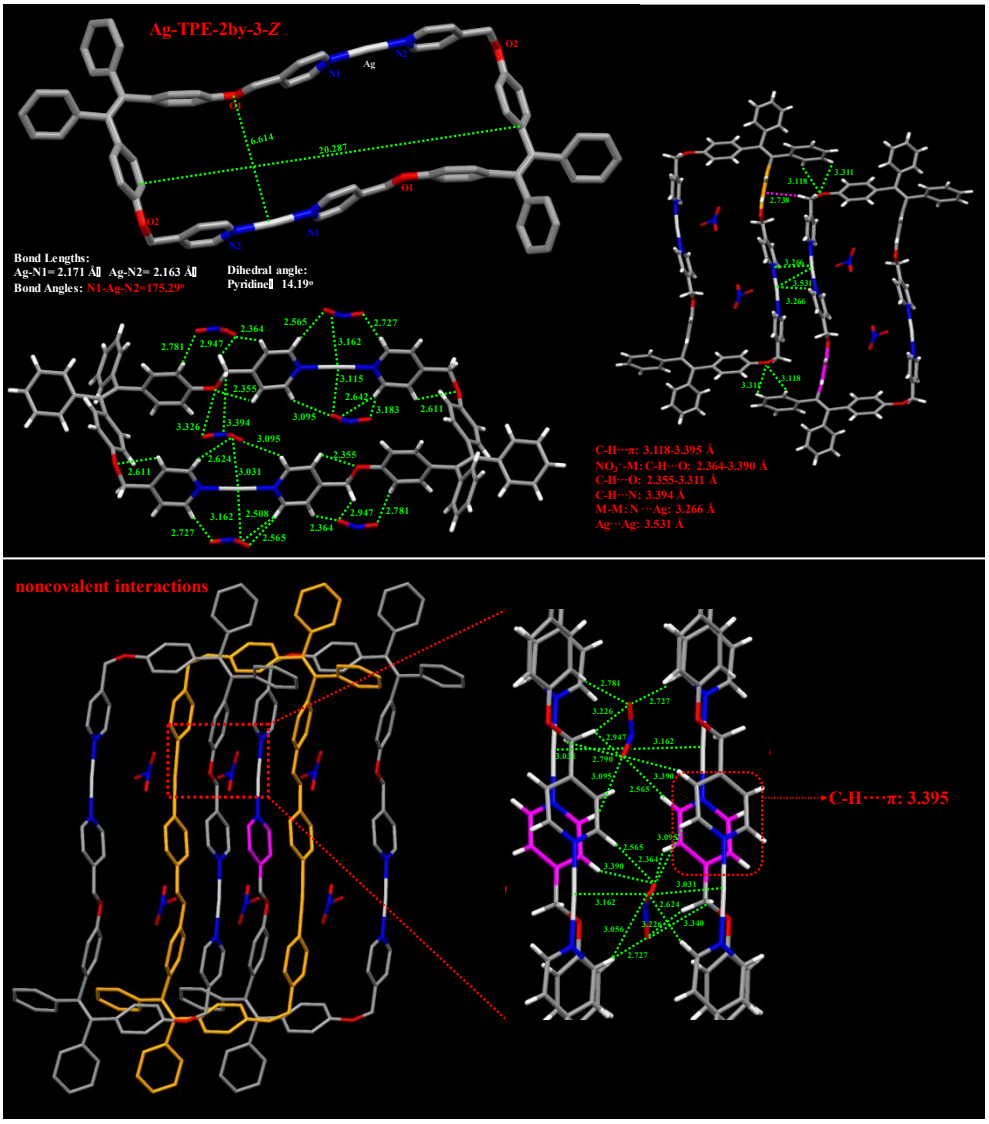

Figure S5. Single crystal structural of **Ag-TPE-2by-3-*Z*** and intermolecular noncovalent interactions.

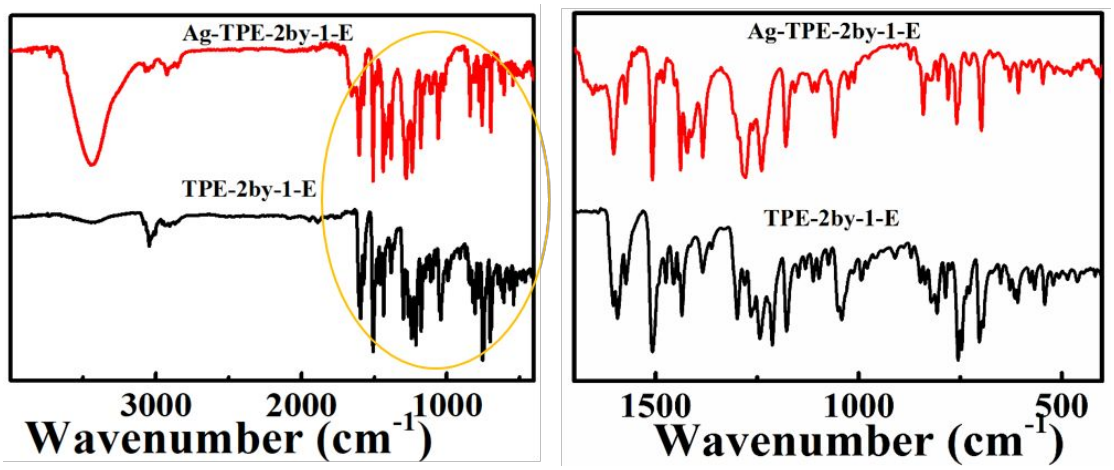

Figure S6. FTIR spectra of **TPE-2by-1-*E*** and **Ag-TPE-2by-1-*E***. (The formation of Ag-N bond lead to significantly increased of the related stretching vibration peaks on the pyridine ring (*e.g.* 3300 cm^{-1} (C-H), 1456 cm^{-1} (C=N), 1384 cm^{-1} (C=C)). At the same time, the spatial distribution of the TPE molecule is limited, which results in a small change in its associated stretching vibration peak. It should be noted that the infrared spectrum at 840 cm^{-1} has a distinct characteristic absorption peak of silver nitrate, which further proves that the Ag coordination polymer **Ag-TPE-2by-1-*E*** was generated).

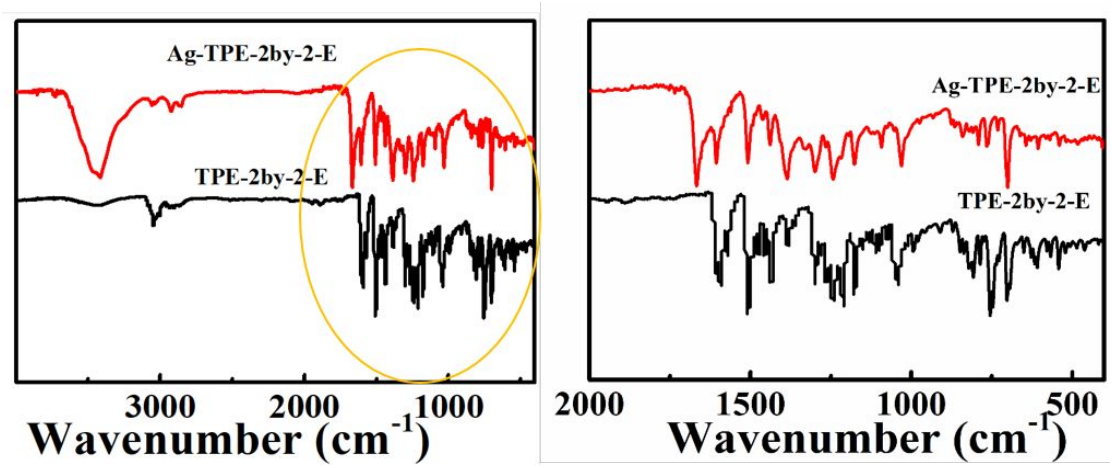

Figure S7. FTIR spectra of **TPE-2by-2-*E*** and **Ag-TPE-2by-2-*E***. (The formation of Ag-N bond lead to significantly increased of the related stretching vibration peaks on the pyridine ring (*e.g.* 3300 cm^{-1} (C-H)), while the out-of-plane bending vibration of the pyridine ring at 786 cm^{-1} weakened bring about the absorption decreased. At the same time, the spatial distribution of the TPE molecule is limited, which leads to a reduction in its associated stretching vibration peaks (1603 cm^{-1}, 1507 cm^{-1}). Especially, a new strong nitro asymmetric stretching vibration peak appeared at 1667 cm^{-1}, which proved that silver nitrate successfully coordinated with the **TPE-2by-2-*E***.)

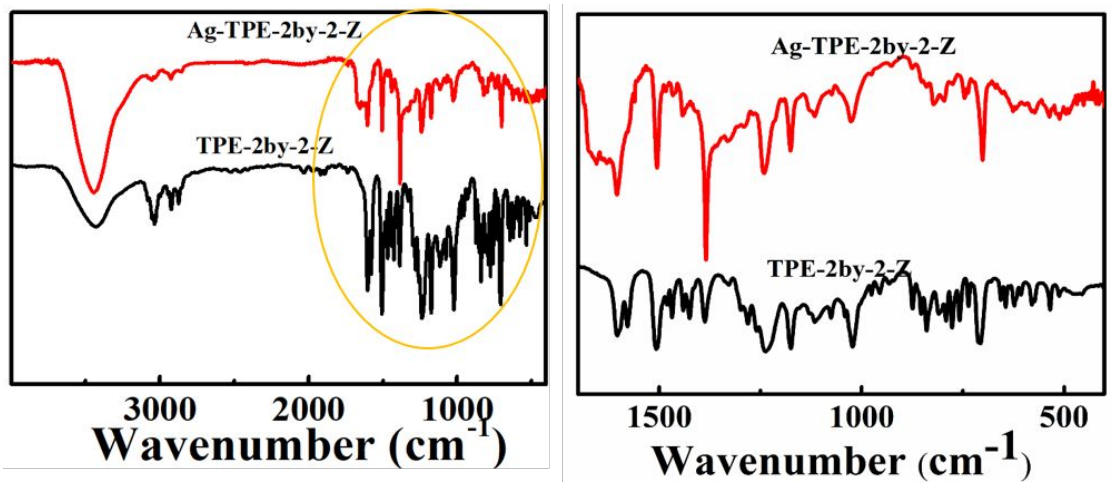

Figure S8. FTIR spectra of **TPE-2by-2-*Z*** and **Ag-TPE-2by-2-*Z***. (The formation of Ag-N bond lead to significantly enhanced of the related stretching vibration peaks on the pyridine ring (*e.g.* 3300 cm^{-1} (C-H), 1384 cm^{-1} (C = C)). At the same time, the spatial distribution of TPE molecules was limited, which bring about a reduction in the stretching vibration peak at 1280 cm^{-1} and a disappearance of the strong absorption peak at 1578 cm^{-1}. Especially, a new strong nitro asymmetric stretching vibration peak appeared at 1654 cm^{-1}, which proved that silver nitrate successfully coordinated with the **TPE-2by-2-*Z*.**)

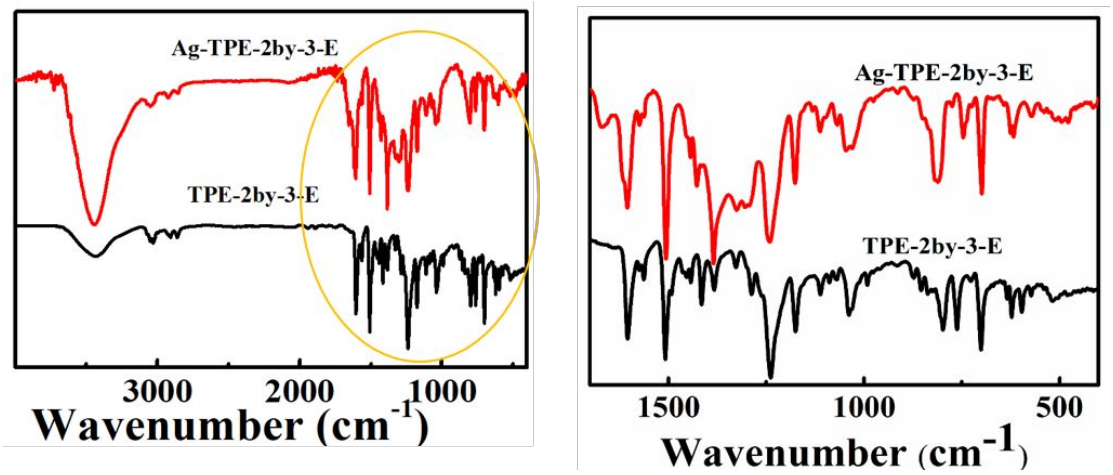

Figure S9. FTIR spectra of **TPE-2by-3-*E*** and **Ag-TPE-2by-3-*E***. (The formation of Ag-N bond lead to significantly enhanced of the related stretching vibration peaks on the pyridine ring (*e.g.* 3300 cm^{-1} (C-H), 1508 cm^{-1} (C = N), 1384 cm^{-1} (C = C)). At the same time, the spatial distribution of TPE molecules was limited, which bring about a reduction in the stretching vibration peak at 1435 cm^{-1} and the disappearance of the strong absorption peak at 1578 cm^{-1}. Especially, a new strong nitro asymmetric stretching vibration peak appeared at 1654 cm^{-1}, which proved that silver nitrate successfully coordinated with the **TPE-2by-3-*E*.**)

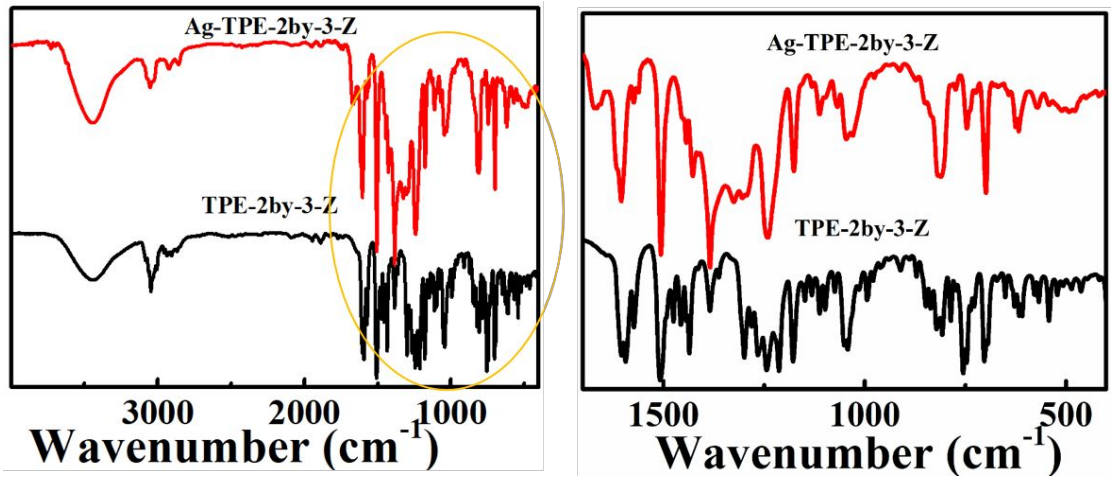

Figure S10. FTIR spectra of **TPE-2by-3-*Z*** and **Ag-TPE-2by-3-*Z***. (The formation of Ag-N bond lead to significantly enhanced of the related stretching vibration peaks on the pyridine ring (*e.g.* 3300 cm^{-1} (C-H), 1508 cm^{-1} (C = N), 1384 cm^{-1} (C = C)). At the same time, the spatial distribution of TPE molecules was limited, which bring about reduction of the stretching vibration peaks at 1562 cm^{-1} and 1439 cm^{-1}. Especially, a new strong nitro asymmetric stretching vibration peak appeared at 1671 cm^{-1}, which proved that silver nitrate successfully coordinated with the **TPE-2by-3-*Z***.)

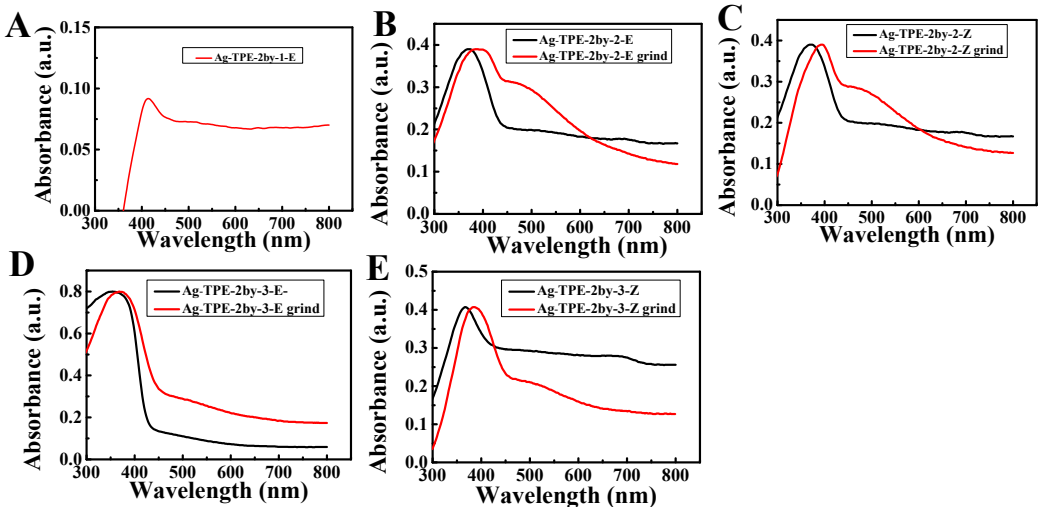

Figure S11. Solid UV absorption of **Ag-TPE-2by-1-*E*** (A), **Ag-TPE-2by-2-*E***(B), **Ag-TPE-2by-2-*Z***(C), **Ag-TPE-2by-3-*E***(D) and **Ag-TPE-2by-3-*Z*** (E): pristine and ground in pristine state.

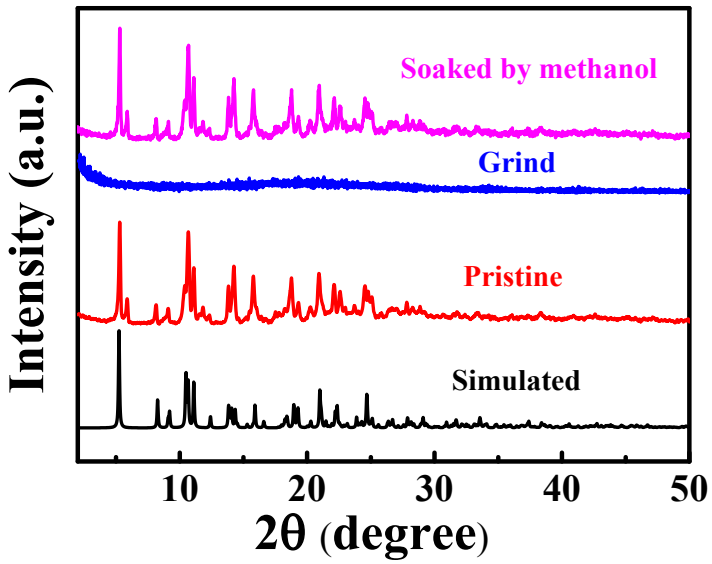

Figure S12. XRD patterns of **Ag-TPE-2by-3-*E***: simulated, pristine, ground and soaked by methanol.

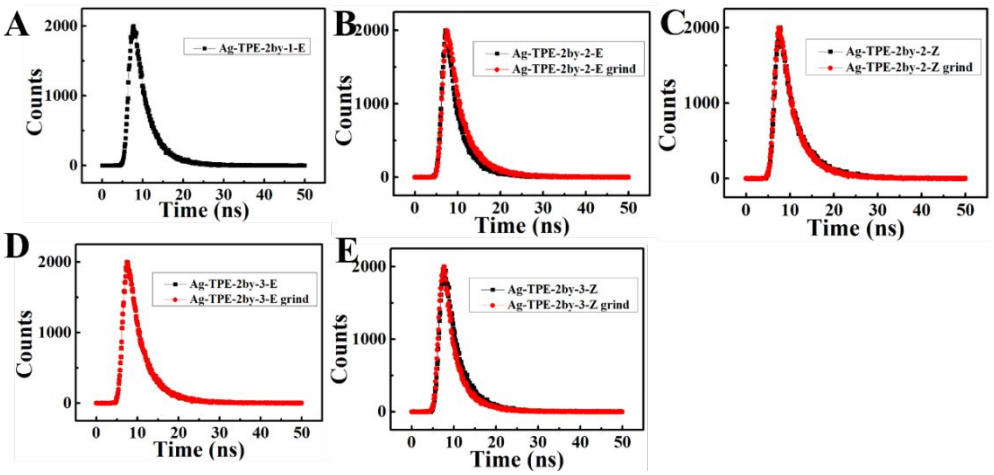

Figure S13. Fluorescence lifetime o**f Ag-TPE-2by-1-*E***(A), **Ag-TPE-2by-2-*E***(B), **Ag-TPE-2by-2-*Z***(C), **Ag-TPE-2by-3-*E***(D) and **Ag-TPE-2by-3-*Z*** (E).

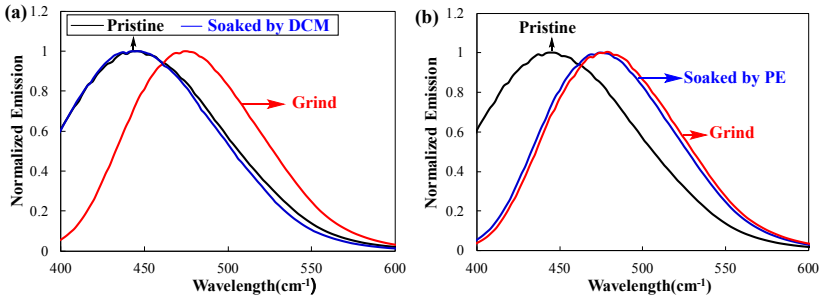

Figure S14. Fluorescence emission spectrum of **Ag-TPE-2by-3-*Z***: (a) soaked by DCM; (b) soaked by PE.

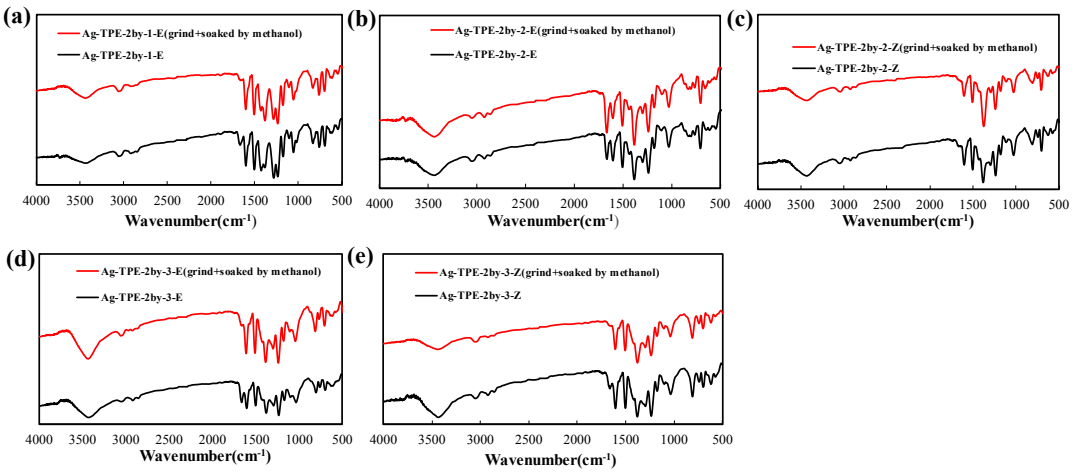

Figure S15. FTIR spectra of **Ag-TPE-2by-1-*E***(a), **Ag-TPE-2by-2-*E***(b), **Ag-TPE-2by-2-*Z***(c), **Ag-TPE-2by-3-*E***(d) and **Ag-TPE-2by-3-*Z***(e), the solid red line is the infrared spectrum of methanol treatment, and the solid black line is the infrared spectrum of the starting sample.